Singlet-State Electron Transfer between a Porphyrin and Ubiquinone: A Transient Resonance Raman and Quantum Chemical Study[1]

Tione Buranda,* Mark Enlow, Jack Griener, Neal Soice, and Mark Ondrias*

The Department of Chemistry, The University of New Mexico, Albuquerque, New Mexico 87131

Received: November 11, 1997; In Final Form: May 5, 1998

Radical ion pairs resulting from bimolecular electron transfer between excited singlet porphyrin donors and quinone acceptors have such short lifetimes that they are rarely observed. Here we report the results of a spectroscopic investigation of the photodynamics of a noncovalent complex of a free base *meso*-tetrakis (4-sulfonatophenyl)porphine (P) and 2,3-dimethoxy-5-methyl-1,4-benzoquinone (ubiquinone, UQ_0). P and UQ_0 form a weak ground-state complex ($K_a \approx 1.0 \times 10^3$ M^{-1}), which decays via a CT intermediate after photoexcitation of a local porphyrin $\pi-\pi^*$ excited state. Transient resonance Raman spectroscopy (TRRS) was employed to identify and characterize singlet-correlated electron-transfer intermediates in this process. The transient porphyrin cation modes are well-characterized and conform to previous assignments. While some of the modes expected of the ubiquinone radical anion are obscured by the porphyrin vibrations, the predominantly C═C and C═O modes are clearly discernible in the transient RR spectra. Ab initio calculations were used to help assign the observed modes of the UQ_0 and calculate "self-exchange" reorganizational energy (≈0.60 eV) for the $UQ_0/UQ_0^{\bullet-}$ radical anion pair. These results are discussed in the context of modern theories of electron transfer.

I. Introduction

The chemically important feature of the primary step in photoinduced electron-transfer (PET) processes is the conversion of electronic energy of an excited state into redox energy.[2] The photosynthetic processes of green plants and bacteria provide an instructive limit of efficient photoinduced charge transfer. In the photosynthetic reaction centers (RC), light-induced charge separation is initiated by photoexcitation of a bacteriochlorophyll complex into its lowest excited singlet state. This is followed by ultrafast charge migration to an intermediate acceptor (a bacteriopheophytin molecule). Rapid and efficient secondary ET to another acceptor (a ubiquinone) creates chemical potential with virtually no energy loss owing to back electron transfer (BET).[3] There is strong interest in understanding the mechanistic details of photosynthetic ET and in exploiting that knowledge to create simpler model systems which convert light into chemically useful energy. Porphyrin-like molecules and naturally occurring quinones play essential electron transport roles in reaction centers, and thus chemical systems containing those species as donors and acceptors in photoinitiated ET have been extensively studied. A successful means of ensuring high quantum yields of ET is to create covalently linked molecular systems[4] designed to undergo efficient PET and maintain a useful lifetime for charge separation. A common problem associated with these systems lies in low synthetic yields and environmental stability of the products. An alternative approach utilizes noncovalently attached systems. A variety of methodologies ranging in complexity from H-bonding motifs[5] to base-pairing strategies[6] have been used, but the simplest model systems have been those relying on diffusive encounters or weak interactions between donor−acceptor pairs in solution.[7]

The remarkable efficiency of charge separation in reaction centers has been traditionally ascribed to favorable Franck−Condon factors.[8] In general, the driving forces ($-\Delta G$) associated with forward ET in RCs are smaller than those associated with the BET process. There is little molecular distortion (and hence reorganization energy (λ)) during ET; thus, large values of $-\Delta G_{BET}$ lead to poor vibrational overlaps, leading to slow BET rates. In contrast, singlet-correlated ET products from diffusional systems have rarely been observed to separate to free ions because of extremely rapid BET.[9] For example, Holten et al.[10] using picosecond flash spectroscopy found that although efficiently quenched by benzoquinone (in acetone:methanol solution), singlet-state bacteriopheophytin does not yield detectible radical ions. The photodynamics of simple bimolecular systems are influenced by their comparatively large reorganizational energies (comparable in magnitude to ΔG_{BET}), which are typically associated with the small quinone acceptor moiety, which undergoes sizable distortions upon ET. Thus an important prequisite for the rational utilization of these model systems as mediators of energy conversion, or reactivity in general, is an understanding of the structural changes associated with ET.

This work concerns itself with the characterization of rarely observed singlet ET intermediates in a system where a porphyrin donor and a ubiquinone acceptor exist in solution equilibrium between free and associated forms. Excitation into either the Soret or Q-band of a porphyrin donor in the absence of an acceptor produces an excited singlet-state S_1. This is followed by prompt intersystem crossing to a long-lived triplet state.[11] The presence of an acceptor in solution may lead to oxidative quenching of either excited state depending on the conditions. In weakly coupled or diffusional systems, electron transfer from the excited singlet state may occur in competetion with intersystem crossing to a triplet state which, owing to spin selection rules, has a much longer lifetime than the singlet state. In the ground-state complex, excited-state reactivity occurs prior to intersystem crossing and this involves singlet intermediates. (Figure 1A).

* To whom correspondence should be directed: buranda@unm.edu or mondrias@unm.edu, FAX 505-272-6995.

10.1021/jp980168v CCC: $15.00
Published on Web 10/09/1998

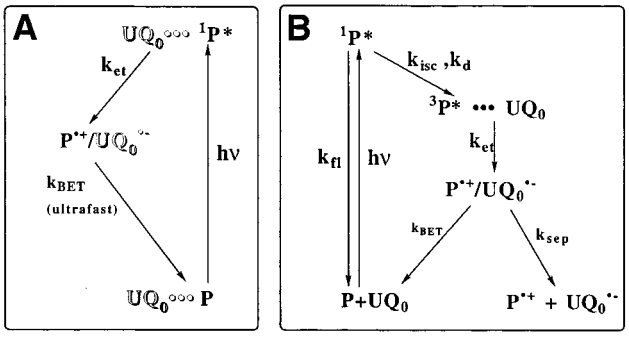

Figure 1. General scheme showing transient decay pathways of porphryin (P) donor and quinone (UQ_0) acceptor photogenerated states. (A) $UQ_0\cdots P$ represents a fraction of complexed or associated P and UQ_0 leading to quenching of the singlet state. $h\nu$ represents laser excitation at 436 nm; k_{et}, k_{BET} are the rate constants of forward and back electron transfer, respectively. (B) Diffusive quenching of the triplet P state, k_{fl} represents singlet flourescence rate contstant, k_{isc} and k_d are the singlet to triplet intersystem crossing and diffusion rate constants, respectively, and k_{sep} is the free ion separation rate constant.

In a previous study[12] we used transient absorption spectroscopy to investigate the dynamics of electron transfer between excited triplet zinc *meso*-tetrakis (4-sulfonatophenyl)porphine (^{3}MP*) and 2,3-dimethoxy-5-methyl-1,4-benzoquinone (ubiquinone, UQ_0). Even though substantial yields of MP π radical cations were observed from the triplet excited-state precursors (owing to spin-forbidden triplet to singlet BET), no evidence of electron-transfer products from the singlet manifold was observed in that study. Quenching of the triplet excited state by the redox partner leads to primary charge-separated species such as exciplexes and solvated geminate radical ion pairs in high yield. In the absence of chemical reactions or other processes within the geminate radical pair, the quantum yield of free ion formation is affected by competetion with first-order back electron transfer (k_{BET} in Figure 1B) and solvation (k_{sep} in Figure 1B).

Here we report the results of using transient resonance Raman spectroscopy (TRRS) to directly observe the PET-generated product species from the singlet manifold in this system. Under favorable conditions TRRS provides a relatively straightforward means of generating and probing intermediate species. Transient absorption spectra tend to be broad and featureless, making it difficult to detect and interpret small changes in optical densities especially in systems with multiple chromophores. In contrast, vibrational spectra are usually well-resolved and provide direct information on the molecular structural changes associated with electron transfer. Our TRRS observations provide the strongest experimental evidence to date, supporting electron transfer as a route to ^{1}P* singlet deactivation in bimolecular systems of this type. Such data is crucial in building suitable model systems since, in part, the efficiency of the photosynthetic reaction center can be traced to the near absence of structural distortions during the early events of photoinduced electron transfer. In addition we have used semiempirical ab initio energy calculations of the neutral ubiquinone/radical anion pair to provide a quantitative description of the molecular reorganization undergone by the acceptor, thus enabling us to explore quantitative limits on the influence of Franck−Condon factors on the efficiency of charge separation. The results of this study are presented in the context of electron-transfer formalisms, and their relevance to ET dynamics in model systems is discussed.

II. Experimental Section

A. Materials. *meso*-Tetrakis(4-sulfonatophenyl)porphine (Porphyrin Products; Logan, UT) and 2,3-dimethoxy-5-methyl-1,4-benzoquinone (Aldrich) were used without further purification.

B. Ground-State Complexes: Absorption Spectroscopy, Fluorescence Quenching. Absorption difference spectra of solutions containing 1×10^{-5} M porphyrin and varying [UQ_0] ($10^{-5} - 10^{-3}$ M) were obtained using an HP8452 diode array spectrophotometer. The absorption data were used to produce a Benisi-Hildebrand[13] plot of the complex absorption near the 460 nm region.

Steady-state luminescence data were obtained with a SLM Aminco 8000 (SLM Instruments, Rochester, NY) fluorescence spectrophotometer. Fluorescence spectra of the porphryin singlet excited state were taken in the presence and absence of UQ_0. Concentrations of the reactants that were used (μM [P] and mM [UQ_0]) spanned the range where diffusive quenching is negligible during the lifetime of the singlet state.

C. Transient Resonance Raman Spectroscopy (TRRS). Single-pulse, transient resonance Raman spectra of P and UQ_0 were collected using protocols described previously.[14] The third harmonic, 355 nm, of a Spectra Physics DCR-2 YAG laser was used to pump a Spectra Physics PDL-2 dye laser (Coumarin 440). A modification of the conventional backscattering geometry was used for the Raman scattering and collection. A laser beam was focused by a lens (spherical or cylindrical) and projected onto the sample with an angle of about 30° from perpendicular to the face of the cuvette. The scattered light was then collected by a camera lens ($f = 75$ mm) that provides short focal length and a large solid angle for light collection. The collected light was then collimated and imaged onto the entrance slit of the spectrometer using a second (*f*-matching) focusing lens. A polarization scrambler was placed directly before the entrance slit of the spectrograph to remove the polarization bias in the efficiency of the dispersing system.

Raman scattered light was collected with a Spex 1403 double-grating (1800 g/mm) spectrograph and detected with a Hamamatsu R928 photomultiplier tube. The detector was interfaced to a gated integrator/boxcar averager (E.G & G. Princeton Applied Research, model 165 gated integrator and model 162 averager), and the signal averaged voltage was sent to an A/D converter interfaced to a 386 PC using Spex software. Raman spectra were collected from neutral aqueous solutions of P, UQ_0, and both P and UQ_0. Ground-state spectra were taken using 0.4 mJ/pulse, and excited-state transients were generated from 2 mJ laser pulses.

D. Ab Initio Studies on Ubiquinone. Ab initio calculations were performed on an IBM RS6000 43P using the Gaussian 94 program suite.[15] Calculations for the neutral molecule were performed at the RHF/6-31G level of theory, while those on the radical anion were performed at the UHF/6-31G level of theory. Additional calculations were performed employing density functional methods[16a,b] (DF) utilizing the BLYP/6-31G-(d) basis sets. Complete geometry optimizations were performed followed by frequency calculations in order to verify that the stationary points obtained were true minima. The frequency calculations were repeated with isotopically labeled carbonyl oxygens (^{18}O) in order to aid in assignment of vibrational modes. Vibrational frequencies obtained were scaled by a factor of 0.89 (0.99 for DF) as suggested by Pople *et al.*[16c] to account for basis set incompleteness, vibrational anharmonicity, and other factors. The resulting molecular orbitals and vibrational modes were then studied with the visualization program Molden.[17]

III. Results

A. Photoinduced Electron Transfer from Porphyrin Excited Singlet. *1. Ground-State Complexes.* The present TRR

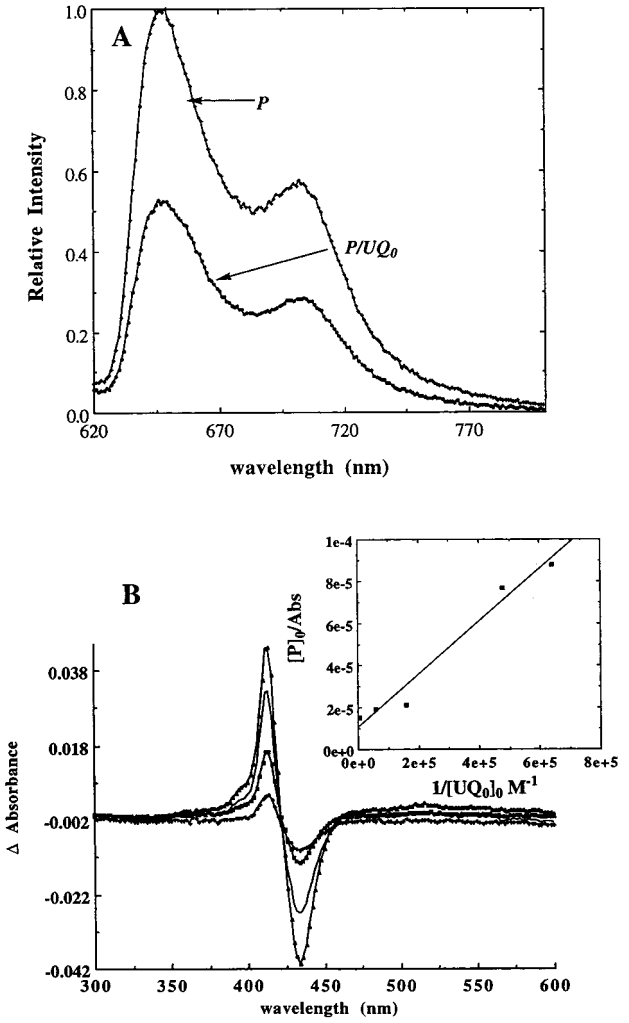

Figure 2. (A) Fluorescence quenching of (10^{-5} M) ^{1}P* by complexed 10^{-3} M UQ_0. (B) Ground-state complex: ground-state absorption spectra, indicating complexation between 10^{-5} M P and [UQ_0] (10^{-6}–10^{-4} M). Insert shows a Benisi−Hilderbrand plot, with $K \approx 10^3$ M^{-1}; see text for details.

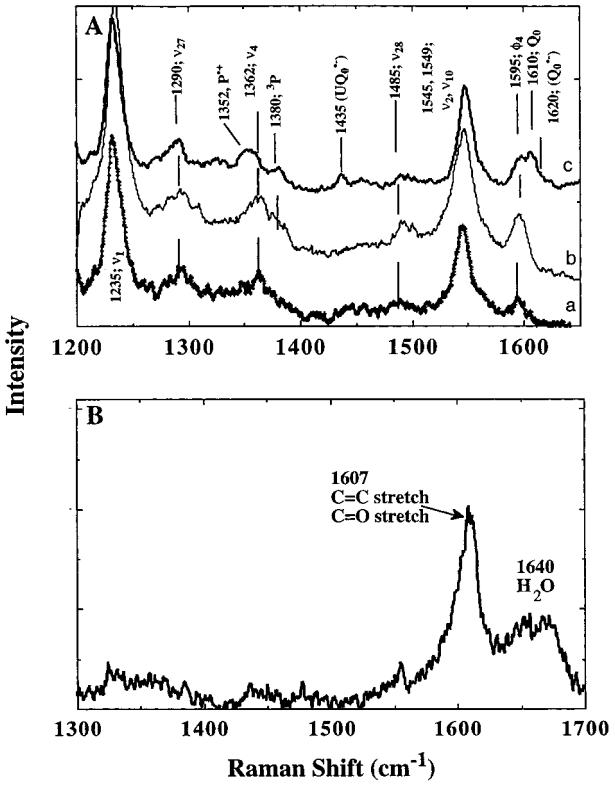

Figure 3. (A) 436-nm Raman spectra as a function of pulse energy; trace a, ground-state resonance Raman spectrum of an aqueous solution of P and UQ_0 (10^{-5} and 10^{-3} M, respectively). The data were collected at 0.4 mJ/pulse; only P vibrational frequencies are observable. Trace b, collected at high laser power (2 mJ/pulse), is of an aqueous solution of P alone. Spectrum shows mixture of ground (S_0) and excited state (S_1, T_1) species; the latter are generated and probed by the same laser pulse. Trace c represents a mixture of (P)S_0, (P)S_1, (P)T_1, and $P^{\bullet+}$/$UQ_0^{\bullet-}$ species modulated by their integrated kinetics within the (2 mJ/pulse) excitation pulse, taken from an aqueous solution of P and UQ_0. (B) 436-nm ground-state Raman spectrum of UQ_0 in aqueous solution.

experiments were designed to probe the electron-transfer dynamics from the porphyrin singlet state. Formation of ground-state complexes enables the UQ_0 to intercept the excited ^{1}P* before intersystem crossing to ^{3}P* can occur. Application of single-pulse TRRS in this case is likely to yield positive results if a reasonable concentration of preassociated complex is present in solution. Fluorescence spectra (Figure 2a) from the ^{1}P* excited state indicate that at least 50% of the excited singlet state is quenched in the presence of UQ_0 owing to formation of ground-state complexes. Complex formation is unequivocally demonstrated by the difference absorption data in Figure 2. The absorption data were analyzed using the standard Benisi−Hildebrand expression[13] for an assumed 1:1 complexation[18]

$$\frac{[P]_0}{\mathrm{Abs}} = \left(\frac{1 + [P]_0 K}{\epsilon K}\right) \frac{1}{[\mathrm{UQ_0}]_0 + \frac{1}{\epsilon}} \qquad (1)$$

where $[P]_0$ and $[UQ_0]_0$ are the initial concentrations of the reactants and Abs is the absorbance measured at 460 nm. The equilibrium constant *(K)* and extinction coefficient (ϵ) were obtained from the slope and intercept of a linear plot of $[P]_0$/Abs versus $1/[UQ_0]_0$ in eq 1. The value of K (1.0×10^3 M^{-1}) is consistent with a substantial level of association in the ground state and is well within the range of values obtained in similar systems.[18b]

2. Transient Resonance Raman Spectroscopy. Resonance Raman spectra obtained with the single-pulse protocol employed in this study reflect the integrated response of the P/UQ_0 over the duration of the excitation pulse.[14] Thus the observation of a given excited state in the transient spectra is strongly dependent on both the photon flux and its relaxation dynamics. Ground and excited-state resonance Raman spectra are shown in Figure 3. Traces b and c were generated and probed by the same 2 mJ laser pulse and consist of a mixture of ground (P), triplet (^{3}P*), and radical ion pairs ($P^{\bullet+}/UQ_0^{\bullet-}$). The respective populations of the species are modulated by their integrated kinetics within the excitation pulse, vide infra. The transient spectra of ^{1}P* + ^{3}P* + $P^{\bullet+}/UQ_0^{\bullet-}$ were resolved from ground-state scattering by subtraction of appropriately scaled (to avoid negative peaks) multiples of the low-power spectrum of the latter. The results are shown in Figure 4. A summary of the vibrational frequencies and their assignments is shown in Table 1.

3. Ab Initio Results on Ubiquinone. (a) Basis Set Effects. The BLYP/6-31G* basis set results were generally acceptable for vibrational and structural information, but, however, the energy calculations were deemed to be less reliable *(*vide infra*)*.[19a] The results given here were obtained using the standard 6-31G split valence basis set. Larger basis sets, including 6-31G* and cc-pVDZ, were also employed but gave unsatisfactory results. Most significantly, C═O bond lengths obtained with these basis sets

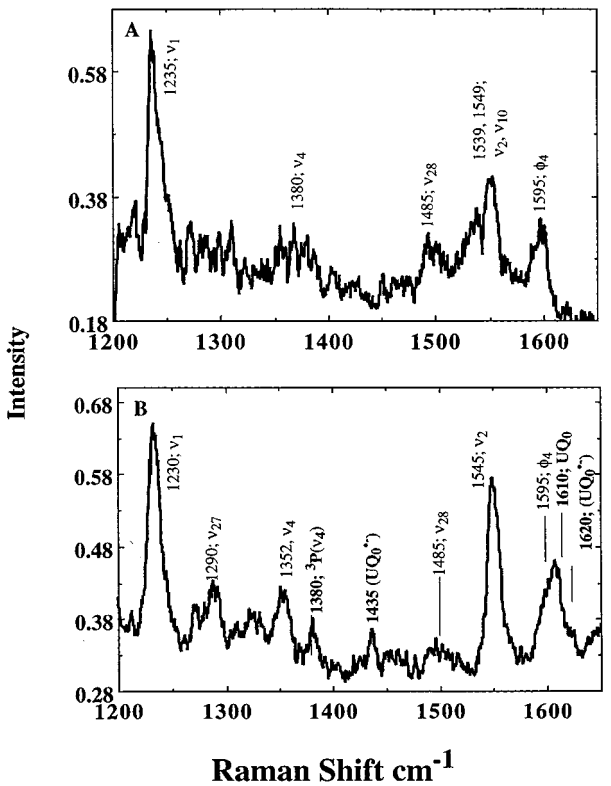

Figure 4. (A) (b − a): Difference transient spectrum of the T_1 state obtained by subtracting the ground-state spectrum appropriately scaled to avoid negative peaks. (B) (c − a): Trace of difference transient $P^{\bullet+}/UQ_0^{\bullet-}$ and (P)T_1 species.

were unrealistically short, being on the order of 1.19 Å. In addition, Hartree−Fock stability calculations revealed instabilities in the molecular wave functions obtained with these larger basis sets. (These deficiencies were not observed in the 6-31G results presented here.) The molecular wave function for the radical anion quinone at the UHF/6-31G level of theory had a S^2 eigenvalue of 1.0145 (a value of 0.75 would indicate a pure doublet state), an indication of significant mixing with the quartet and higher multiplicity states. While moderate spin contamination has been observed in the UHF wave function of the radical anion, previous studies on this[19b] and similar systems have shown negligible effects on the results.[19c,d]

(b) Geometrical Structure. The optimized equilibrium geometries obtained were of C_1 symmetry. The two methoxy side chains are rotated out of the plane of the ring in differing directions, thus breaking the possible C_s symmetry. This geometry is observed in both the neutral and radical anionic species. A partial list of geometric parameters for both the neutral and the radical anion species is given in Table 2. Results of BYLP/6-31G* basis sets are included as part of the Supporting Information (Table 2S). A 3D contour plot of the LUMO of the neutral molecule is given in Figure 5 and is consistent with a previous result.[19d] This orbital is bonding with respect to the C−C bonds and antibonding with respect to the C═C and C═O bonds. Thus addition of an electron to the orbital results in the increase of C═C and C═O bond lengths, which is accompanied by a concomitant decrease in the C−C bond lengths.

The total energy of the neutral ubiquinone at its equilibrium geometry, $E(UQ_0)$, and at the equilibrium geometry of the radical anion, $E(UQ_0^*)$, were −645.7356 au and −645.7121 au respectively (1 au = 27.12 eV). The total energy of the radical anion ubiquinone at its equilibrium geometry, $E(UQ_0^{\bullet-})$, and at the equilibrium geometry of the neutral, $E(UQ_0^{\bullet-*})$, were

TABLE 1: (A) Raman Frequencies of S_0, T_1, and $P^{\bullet+}$ States of H_2TPPS_4 Measured in This Work Compared to Literature Ground-State H_2TPP Frequencies and (B) Ubiquinone Vibrational Frequencies

(A)

		$H_2(TPPS)^c$		
assignment[a]	typical[b] TPP	S_0	T_1	$P^{\bullet+}$
ν_1 $\nu(C_m\phi)$	1234	1236	1235	1230
ν_2 $\nu(C_\beta C_\beta)$	1546	1550	1539	1545
ν_3 $\nu(C_\alpha C_m)$sym.	1425			
ν_4 ν(pyr 1/2-ring)$_{sym.}$	1360	1362	1380	1352
ν_{10} $\nu(C_\alpha C_m)_{asym.}$	1610	1595		1549
ν_{11} $\nu(C_\beta C_\beta)$	1493		1495	
ν_{12} ν(pyr 1/2-ring)$_{sym.}$	1353			1320
ν_{27} $\nu(C_m\phi)$	1270	1290		1290
ν_{28} $\nu(C_\alpha C_m)_{sym.}$	1485		1485	1485

(B)

assignment[d]	UQ_0	$UQ_0^{\bullet-}$	$UQH_0^{\bullet}$ [f]
$C{=}C_{str}$(8a)	1608	1618	1506
$C{=}O_{str}$(7a)	1608	1608	
$C{=}O_{str}$(7a)		1435 (1)	
$C{=}C_{str}$(8b)		1527	1617
$C{-}C_{str}$(14)		1305 (2)	

[a] Kitagawa, T.; Abe, M.; Kyogoku, Y. *J. Chem. Phys.* **1978**, *69*, 4516. [b] Li, X.; Zgierski, M. Z. *J. Phys. Chem.* **1991**, *95*, 4268. [c] This work. [d] Mode assignments based on the work of (i) Tripathi, G. N. R. *J. Chem. Phys.* **1981**, *74*, 6044. (ii) Beck, S. M.; Brus, L. E. *J. Am. Chem. Soc.* **1982**, *104*, 4789. (iii) Parker, A. W.; Hester, R. E.; Phillips, D.; Umapathy, S. *J. Chem. Soc., Faraday Trans.* **1992**, *88*, 2649. [e] Semiquinone frequencies measured in this work: (1) this number is 39 cm^{-1} less than that reported by Parker et al. in an isolated $UQ_0^{\bullet-}$ (2) values from Parker, A. W.; Hester, R. E.; Phillips, D.; Umapathy, S. *J. Chem. Soc., Faraday Trans.* **1992**, *88*, 2649. [f] Values from Parker et al., see footnote *e* (1).

−645.7850 au and −645.7655 au, respectively. The relationship between these energies, their differences, and structural changes associated with the reduction process are illustrated in Figure 6 and are discussed below. Results of BLYP/6-31G* basis set are tabulated in Table 4S of the Supporting Information; it has been previously shown[19a] that this basis set tends to underestimate electron affinities of similar systems (e.g., *p*-benzoquinone, where experimental data is available). In our case the HF/6-31G basis gives an adiabatic electron affinity of 1.34 eV (Figure 6), whereas the BLYP/6-31G* result is 1.24 eV. We believe the HF value to be a better estimate, based on the known value (1.63 eV) of the closely related trimethyl-*p*-benzoquinone.[19a] The methoxy groups of ubiquinone make it harder to reduce than trimethyl-*p*-benzoquinone; thus, the putative electron affinity of the former is expected to be lower than 1.63 eV.

(c) Vibrational Frequencies. A partial list of scaled vibrational frequencies along with isotopic shifts ($\Delta = \nu^{18}O - \nu^{16}O$) and assignments is presented in Table 3. Results of BYLP/6-31G* basis sets are included as part of the Supporting Information (Table 3S). These assignments are based on displacement vectors obtained from the frequency calculations and the magnitudes of the isotopic shifts. In most cases, modes involving bond stretching were strongly coupled, making assignments to a single internal coordinate impossible. The assignments given here should be taken as a qualitative description of the primary characteristic of each mode. The isotopic shift may be used as an estimate of the amount of C═O stretching involved in a particular mode.

(d) Electronic Distribution. The extent of localization of the additional electron about a particular carbonyl group can be estimated from the change in carbonyl bond lengths and from changes in partial atomic charges associated with each atom.

TABLE 2: (A) Partial List of Optimized Geometric Parameters[a] for Ubiquinone (UQ_0) (Experimental Numbers in Parentheses from Reference 35) and Ubiquinone Radical Anion ($UQ_0^{\bullet-}$) and (B) Partial Atomic Charges for Ubiquinone (UQ_0) and Ubiquinone Radical Anion ($UQ_0^{\bullet-}$) As Obtained from a Mulliken Population Analysis of RHF/6-31G and UHF/6-31G Calculations

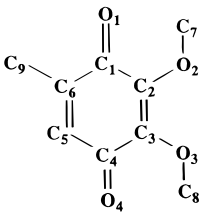

(A)

bond	U	$U^{\bullet-}$	Δ
C_1-C_2	1.483 (1.471)	1.434	−0.049
C_2-C_3	1.328 (1.363)	1.365	+0.037
C_3-C_4	1.480 (1.469)	1.437	−0.043
C_4-C_5	1.487 (1.464)	1.425	−0.062
C_5-C_6	1.331 (1.338)	1.370	+0.039
C_6-C_1	1.470 (1.499)	1.431	−0.039
C_1-O_1	1.219 (1.225)	1.286	+0.067
C_2-O_2	1.359 (1.338)	1.386	+0.027
C_3-O_3	1.360 (1.357)	1.383	+0.023
C_4-O_4	1.218 (1.242)	1.278	+0.060
O_2-C_7	1.446 (1.423)	1.433	−0.013
O_3-C_8	1.445 (1.464)	1.431	−0.014
C_6-C_9	1.500 (1.498)	1.507	+0.007

(B)

atom	UQ_0	$UQ_0^{\bullet-}$	Δ
C_1	0.40	0.35	−0.05
C_2	0.33	0.30	−0.03
C_3	0.34	0.29	−0.05
C_4	0.42	0.32	−0.10
C_5	−0.21	−0.22	−0.01
C_6	0.01	−0.03	−0.02
C_7	−0.14	−0.11	+0.03
C_8	−0.14	−0.11	+0.03
C_9	−0.45	−0.44	+0.01
O_1	−0.51	−0.75	−0.24
O_2	−0.73	−0.77	−0.04
O_3	−0.74	−0.74	+0.00
O_4	−0.52	−0.59	−0.07

[a] All units in angstroms. Hydrogen atoms are omitted. Numbers on structure at top refer to numbering scheme used to describe ubiquinone.

Changes in bond length are easily determined from the optimized geometries (Table 2). Partial atomic charges are obtained from a Mulliken population analysis of the molecular wave function. Table 2B lists the resulting partial atomic charges for the neutral and radical anion.

The change in bond length for the C_1-O_1 pair is +0.067 Å, while this quantity for the C_4-O_4 pair is +0.060 Å. The sum of the change in partial atomic charges for the carbonyl group formed by C_1 and O_1 is −0.29, while this quantity for the carbonyl group formed by C_4 and O_4 is −0.17. These observations suggest greater localization about the C_1-O_1 group.

V. Discussion

Bimolecular ET involving excited singlet porphyrin donors and organic acceptors typified by quinones has been studied extensively in the past two decades.[7a] The common thread throughout most of these studies has been the lack of detectable radical ion pairs because of ultrafast BET. In this work we have used transient resonance Raman spectroscopy to characterize the $^1P^{\bullet+}/UQ_0^{\bullet-}$ radical ion products of the photoinitiated ET reaction. The vibrational frequencies are generally consistent with literature values from electrochemically ($P^{\bullet+}$) or photochemically ($UQ_0^{\bullet-}$) generated species. There are, however, some differences in the $UQ_0^{\bullet-}$ frequencies, which may be attributed to the form of the "encounter complex". These "structural" features, which are reflected by the frequency changes from neutral ground-state to charge-separated intermediates, within the ET complex, help identify the important molecular functional groups largely involved in controlling the rates of electron transfer. We have used the data from ab initio calculations of $UQ_0/UQ_0^{\bullet-}$ to show how the ubiquinone centered structural distortions lead to the ultrafast BET rates.

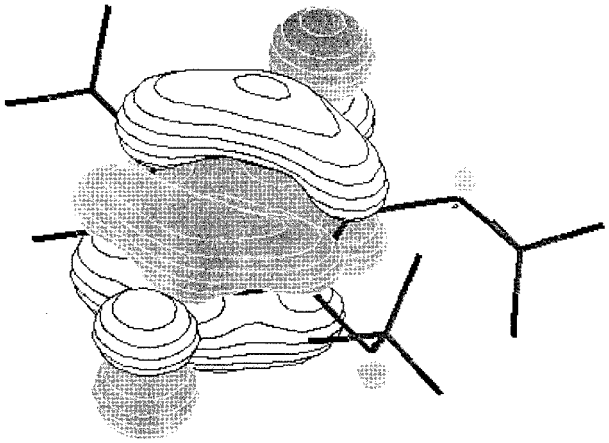

Figure 5. Molecular orbital contour plot ($\Psi = \pm 0.05$) of the LUMO of ubiquinone as obtained by a RHF/6-31G calculation.

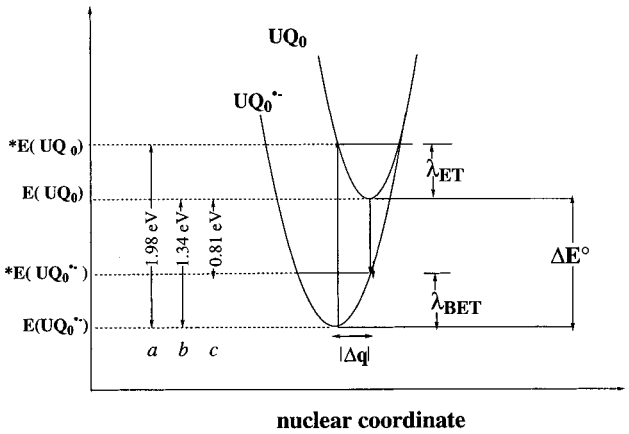

Figure 6. Illustration of the scheme used to calculate intermolecular reorganization energy. *a* refers to vertical ionization energy of $UQ_0^{\bullet-}$; *b* is the adiabatic electron affinity of UQ_0; *c* is the vertical electron affinity of UQ_0. λ_{ET} and λ_{BET} are nuclear reorganizational energies associated with the forward (i.e., UQ_0 reduction) and back electron transfer processes.

A. Excited-State Dynamics and Single-Pulse Resonance Raman Spectroscopy as a Probe For Transient Species. The study of transient species using single-pulse TRRS protocol has been described previously.[14] For clarity some relevent details will be summarized here. In the transient resonance Raman experiments, two photons are required to interact with a given molecule for the transient to be observed: one to initiate transient process and another to probe the intermediates and products via Raman scattering. The small lifetime of the charge-transfer state ($\ll$1 ns)[9] enables the 10 ns laser pulses used here to create a significant population of short-lived excited molecules under quasi-steady state conditions. The incident laser flux

TABLE 3: Calculated Frequencies, Isotopic Shifts (∂), and Qualitative Assignments for Ubiquinone and Its Radical Anion As Obtained by RHF/6-31G and UHF/6-31G Calculations

ubiquinone			ubiquinone radical anion		
frequency	∂	assignment	frequency	∂	assignment
1159	0	$O_2-C_7-H + O_3-C_8-H$ bend	1161	0	O_2-C_7-H bend
1177	1	$O_2-C_7-H + O_3-C_8-H$ bend	1166	2	O_3-C_8-H bend
1206	1	in-plane ring distortion	1192	1	O_3-C_8-H bend
			1214	2	in-plane ring distortion
1265	1	in-plane ring distortion	1279 (1305)	7	in-plane ring distortion
			1342	**11**	**$C_4=O_4$ stretch**
1304	1	C_4-C_3 str + C_4-C_5 asym. str	1393	1	C_6-C_9-H bend
			1408	0	in-plane ring distortion
1346	1	C_1-C_2 str + C_1-C_6 asym. str	1418	0	$O_2-C_7-H+ O_3-C_8-H$ sym. bend
1415	0	C_6-C_9-H bend	**1443 (1474)**	**7**	**$C_1=O_1$ stretch**
1437	0	$O_2-C_7-H + O_3-C_8-H$ sym. bend	1453	2	$H-C_9-H$ bend
1448	0	$O_2-\mathbf{C_7}-H + O_3-C_8-H$ asym. bend	1455	2	$H-C_9-H$ bend
1452	0	$H-C_9-H$ bend	1467	0	$H-C_9-H$ bend
1458	0	$H-C_9-H$ end	1472	3	$H-C_7-H$ bend
1471	0	$H-C_8-H$ bend	1474	0	$H-C_8-H$ bend
1472	0	$H-C_7-H$ bend	1484	0	$H-C_8-H$ bend
1479	0	$H-C_7-H$ bend	1490 (1527)	0	$C_2=C_3$ str + $H-C_8-H$ bend
1481	0	$H-C_8-H$ bend	1500	0	$H-C_7-H$ bend
1646 (1608)	**20**	**sym. $C=O + C_5=C_6$ str**	1533 (1617)	1	$C_5=C_{6\ str}$
1672	6	$C_2=C_3$ str			
1680	**31**	**C=O asym. str**			
1721 (1660)	7	C=C sym. str			

[a] Experimental values from refs 26 and 29 are given in parentheses. All units in reciprocal centimeters.

determines the average time interval between the "pump" and "probe" photons within a laser pulse. If the initial relaxation is rapid on the time scale of this incident laser pulse (i.e., 10 ns), the distribution of electronic and vibrational states in the population that is probed by Raman spectroscopy is expected to be sensitive to the incident laser pulse flux. At low flux, the molecules that are excited throughout the duration of the pulse have, on average, sufficient time to relax prior to being probed and thus yield vibrational bands corresponding to the ground-state equilibrium species. At higher laser fluence, the relaxing molecules are, on average, probed before they can relax, and the resulting spectrum reflects the net contributions from the P/UQ_0 system in various forms of excited as well as ground states.

Electronic properties of excited-state species play pivotal roles in the transient resonance Raman interpretation of porphyrin electronic spectra. These excited states are usually identified with reference to the Gouterman[20] model. In this scheme, the porphyrins are treated as delocalized π systems with a pair of close lying HOMOs of $a_{1u}(\pi)$ and $a_{2u}(\pi)$ symmetry in the idealized D_{4h} point group and a degenerate pair of LUMOs of $e_g(\pi^*)$ symmetry. Degenerate orbital excitations to $a_{1u}(\pi)e_g(\pi^*)$ and $a_{2u}(\pi)e_g(\pi^*)$ configurations result in two singlet transitions that mix via configuration interaction to give the characteristically weak Q-band at 500−650 nm and a strongly allowed B-band transition in the near-ultraviolet (380−450 nm).[20] Electron density MO arguments centered around the β, α, and m positions (Figure 7) have been key in vibrational spectral characterizations of the porphryins *(*vide infra*).* Successful application of TRRS to monitor photoexcited transients ($^3P^*$, $P^{\bullet+}$) is dependent on being in resonance with the relevant species' absorption. Excitation ($^1P \rightarrow {}^{1,3}P^*$), oxidation, or reduction of the porphryin is understood not to perturb the electronic system sufficiently to obliterate the four orbital nature of the electronic transitions in the excited or charged species.[20b] Triplet absorptions are red-shifted with respect to the ground-state absorptions while cationic B-band transitions are typically blue-shifted with respect to the neutral ground-state absorption bands. The 436 nm laser excitation is the best compromise for acceptable resonance conditions with the various porphyrin transients as well as the UQ_0 radical anion.

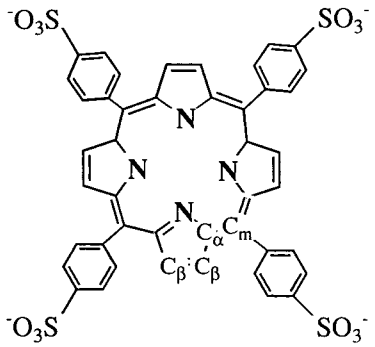

Figure 7. *meso*-Tetrakis (4-sulfonatophenyl)porphine showing functional C-positions, viz, β, beta; α, alpha; and m, meso.

B. Transient Resonance Raman Spectral Analysis. *1. Porphyrin Excited States.* The Raman spectrum of P obtained at low excitation power (shown in Figure 3A (a)) is comparable to the usual ground-state tetraphenylporphyrin spectra reported in the literature, and the modes have been assigned accordingly.[21] Thus, preassociation has little or no effect on the ground-state P spectra. Extensive investigations of metalloporphyrin S_0, S_1, and T_1 states and $P^{\bullet-}$ and $P^{\bullet+}$ radicals have resulted in widely accepted characterizations of vibrational spectra of the neutral and charged ground and excited species of various porphyrins.[21] Electrochemically generated species have been used to provide data on radical ions, and, to the best of our knowledge there are very few reported examples of transient spectra obtained from photoinduced electron-transfer products involving porphyrins.[22,14c]

The putative electron transfer within the 10 ns laser pulse occurs from the preassociated donor acceptor pairs whereas most of the uncomplexed $^1P^*$ undergoes intersystem conversion ($k_{isc} \approx 5.0 \times 10^8\ s^{-1}$) to the triplet state ($T_1$). The T_1 state should remain unquenched on a <10 ns time scale owing to diffusion-limited kinetics. Therefore the transient spectra of solutions containing $^1P^*/UQ_0$ always exhibit features due to the T_1 state (e.g., ν_4 at 1380 cm^{-1} in Figure 4B) as well as the expected $P^{\bullet+}/UQ_0^{\bullet-}$ radical ion pair spectra. Much is already known about the T_1 (and S_1) spectra of the porphyrins. [21] Figure 4A depicts

the spectrum of the T_1 state and may also contain features due to the S_1 state (S_1 and T_1 states are expected to have the same mode frequencies due to similar orbital occupancies).[21d] In contrast, the $P^{\bullet+}$ species is expected to exhibit significant shifts in its vibrational frequencies. The a_{2u} orbital (HOMO in D_{4h} symmetry meso substituents) has most of its electron density at the meso carbons and at the pyrrole nitrogens; the $C_\alpha N$ bonds have strong antibonding character, whereas the $C_\beta C_\beta$ bonds are bonding (Figure 7). The e_g* LUMO orbitals are slightly antibonding at the $C_\beta C_\beta$ positions. It is therefore possible to predict, for example, that the photoinduced S_0: $(a_{2u}(\pi)^2) \rightarrow S_1,T_1$: $(a_{2u}(\pi)e_g(\pi^*))$ transition weakens the $C_\beta C_\beta$ bonds, producing a concomitant downward shift in the vibrational frequency shift of the associated modes (e.g., ν_2 mode frequency changes from 1550 to 1539 cm^{-1}). Conversely removal of electron density from antibonding MOs should cause an upshift in frequencies of the relevant vibrational modes. [21a] The Raman shifts observed in this study are in general agreement with literature values for $P^{\bullet+}$ species and are consistent with the anticipated vibrational behaviour of $P^{\bullet+}$ species (vide infra).

On the basis of thermodynamic considerations ($\Delta G_{ET} = -0.70$ eV),[23] triplet-state data,[12,7a] and other precedents in similar model systems,[9] electron-transfer quenching of the singlet state is likely. The high-power transient spectrum of the P/UQ_0 system contains bands that cannot be ascribed to $^3P^*$ or P but are consistent with the oxidized porphyrin radical cation. Figure 4B represents the transient spectrum of the $P^{\bullet+}/UQ_0^{\bullet-}$ pair obtained by subtraction of appropriately scaled multiples of the low-power spectrum (a in Figure 3A) from the transient spectrum (c in Figure 3A). The difference spectrum displays appreciable frequency downshifts (5−10 cm^{-1}), for the in-plane macrocycle modes. For instance, oxidation of a porphyrin is commonly associated with a shift to lower frequency at "the oxidation state marker" mode ν_4 as indicated by the typical $\Delta\nu$ of −8 cm^{-1}. Further corroborating evidence for the existence of a porphyrin π radical cation is implicated by the changes in the relative intensities of the ν_1 (1230 cm^{-1}) and ν_2 (1249 cm^{-1}) compared to the ground-state or the triplet difference spectra. These undoubtedly arise from changes in the resonance conditions between P and $P^{\bullet+}$ since Soret absorption band of the latter is blue-shifted (15 nm)[12] with respect to the neutral species. We see no evidence for significant structural distortions of the P during ET as the $P^{\bullet+}$ modes are quite similar to those of equilibrium cations generated electrochemically.[21]

2. Ubiquinone. Figure 4B also contains features (most notably bands at 1620 and 1435 cm^{-1}) that are not present in the spectra of P, $^3P^*$, UQ_0 or expected from $P^{\bullet+}$. These have been assigned to the ubiquinone radical anion. It is useful to note that protonated semiquinone radicals, $UQ_0H^{\bullet}$, can be formed via hydrogen abstraction from protic solvents by excited $^3UQ_0$. [24] However, such reactions have been shown to occur on the $10^{-6} - 10^{-8}$ s^1 time scale, which is outside the temporal regime of our single-pulse experiment. Thus we conclude that the radical species observed in this work arise solely from photoinduced electron transfer. The characterization of quinones in their different redox and protonation states continues to be the subject of sustained interest.[25−29] Resonance Raman spectroscopy has been employed to characterize the structural features of a number of quinones including the ubiquinone used in this work.[26] Vibrational assignments are summarized in Table 1B. The neutral ubiquinone, UQ_0 (S_0), spectrum is simple, with only one, resolved band at 1607 cm^{-1} corresponding to accidental degeneracy of the symmetric stretch of the C═C ring bonds and the symmetric combination of the two C═O stretches. Reduction of UQ_0 to form the semiquinone radical anion yields a nine π electron system, producing strong electronic transitions near 420 and 440 nm compared to the single less intense band at 406 nm in the neutral species, (neutral ubiquinone $\epsilon \approx 5300$ M^{-1} cm^{-1} at 425 nm and semiquinone radical $\epsilon \approx 8600$ M^{-1} cm^{-1} at 440 nm).[27] As a result, the absorption cross section for the semiquinone radical $UQ_0^{\bullet-}$ in this (436 nm) region of the Raman probe is substantially higher than that of the neutral ground state. The transition at 440 nm has been assigned as one of $\pi-\pi^*$ character; [28] this leads to resonant enhancement for the associated C═C stretch of $UQ_0^{\bullet-}$ at 1618 cm^{-1} and C═O stretch at 1435 cm^{-1}. While some of the bands previously reported for $UQ_0^{\bullet-}$ may be obscured by interference from the $P^{\bullet+}$ radical cation, it is gratifying to note that the key $UQ_0^{\bullet-}$ bands (1435, 1608, and 1618 cm^{-1}) are easily discernible in the midst of the more prominent $P^{\bullet+}$ vibrations (Figure 4B). In contrast to the $P^{\bullet+}$ spectrum, large structural distortions may be inferred from the C═O frequency, which undergo a 175 cm^{-1} shift upon reduction.

The ab initio results indicate that the LUMO of UQ_0 is antibonding (Figure 5) with respect to the C═C and C═O bonds but bonding with respect to the C−C bonds. Thus, negative changes in vibrational frequencies for the C═C and C═O bonds are expected, while an increase in the frequencies associated with the C−C bonds is anticipated. The ab initio calculations allow access to vibrational frequencies that may not be experimentally observed (Table 3). Experimental numbers from the literature are included where possible. Where comparisons can be made, the agreement between experimentally observed and calculated frequencies is good, being on the order of 30 cm^{-1}, viz: $1608_{sym.C=O+C=Cstr}$. (exp), 1646 cm^{-1} (calc) neutral; $1474_{C=0str}$ (exp), 1443 cm^{-1} (calc) *anion*. The notable exception is the largely $C{=}C_{sym.str}$, which is seen to differ by almost 100 cm^{-1} i.e., 1660 cm^{-1} (exp), 1721 cm^{-1} (calc) and 1617 cm^{-1} (exp), 1533 cm^{-1}(calc) for the neutral and radical anion, respectively. Many of the modes arise from coupled molecular coordinates, the C═C frequencies having some components of C═O character. Our observation of a C═O stretch at ≈1435 cm^{-1} varies from those reported for other quinone anions (1474 cm^{-1}) and strongly suggests some environmental pertubation of that mode.[29] Perhaps the most relevant precedent to this finding can be found from the work of Breton et al.[29a] Photoreduction of ubiquinone in reaction centers was investigated using difference FTIR spectroscopy. In these studies the C═O frequency of a reaction center situated quinone was reported to be lower than that of an isolated ubiquinone. This was attributed to hydrogen bonding of the carbonyl to protein residues within the reaction center. In the present study, it is possible for H-bonding interaction to occur between the $UQ_0^{\bullet-}$ and acidic protons at the nitrogens on the porphyrin macrocyclic core. Thus, the close proximity of the $P^{\bullet+}$ radical may produce carbonyls with less double-bond character and a concomitantly lower frequency.

C. Concerning Structural Distortions and Implications For Back Electron Transfer. Current theories treat nonadiabatic electron transfer as a radiationless process with a golden-rule type expression for the rate constant, as a product of the electronic matrix element squared (V^2) and a Franck−Condon weighted density of states (FCWD). [2,3] The FCWD term contains the dependence on the energy gap, the solvent reorganization (λ_s), and internal molecular reorganization (λ_v) energies. The original formulation of Marcus[8a] was cast in the adiabatic limit (large V) of the ET process where the ability of the system to convert electronic to vibrational energy (typically

TABLE 4: Effect of Franck−Condon Factors on k_{BET} for Ubiquinone (UQ_0) and Bacteriophiophytin (BPh) Acceptors

	UQ_0[a]				BPh[g]			
j[b]	F_j[c]	κ_j[d]	H_j[e]	k_{BET} (s^{-1})[f]	F_j[h]	κ_j[i]	H_j[j]	κ_{BET} (s^{-1})[k]
0	0.15	2.0×10^{-4}	45.0	2.6×10^{8}	0.59	3.3×10^{-24}	433.0	6.5×10^{-12}
1	0.29	0.01	85.0	1.7×10^{10}	0.31	1.7×10^{-16}	231.0	3.0×10^{-4}
2	0.27	0.22	80.0	2.7×10^{11}	0.08	2.5×10^{-10}	61.6	4.8×10^{2}
3	0.17	0.90	50.0	1.1×10^{12}	0.01	1.1×10^{-5}	11.0	1.8×10^{7}
3	**0.17**	**0.90**	**3.1***	$\mathbf{8.2 \times 10^{11}}$				
3	**0.17**	**0.90**	**0.5***	$\mathbf{3.5 \times 10^{11}}$				
4	0.08	0.82	23.0	1.0×10^{12}	2.0×10^{-3}	0.02	1.5	1.1×10^{10}
5	0.03	0.20	9.0	2.2×10^{11}	2.0×10^{-4}	0.70	0.2	6.4×10^{10}
5					$\mathbf{2.0 \times 10^{-4}}$	**0.60**	**0.009***	$\mathbf{4.6 \times 10^{9}}$
5					$\mathbf{2.0 \times 10^{-4}}$	**0.60**	$\mathbf{6.0 \times 10^{-4}}$*	$\mathbf{7.3 \times 10^{8}}$
6	0.01	0.10	2.7	1.0×10^{10}	1.9×10^{-5}	0.02	0.01	7.7×10^{9}
7	2.0×10^{-3}	1.5×10^{-4}	0.7	8.1×10^{7}	1.4×10^{-6}	2.5×10^{-5}	0.001	2.1×10^{7}

[a] Ubiquinone acceptor BET dynamics. [b] BET relaxation channel. [c] $F_j = (e^{-s}\, S^j)/j!$; $S = \lambda_v/(h\nu)$; $\lambda_v = 0.35$ eV, $h\nu_v = 1500$ cm^{-1}. [d] Marcus activation exponential term in eq 4a. $\Delta G = -1.15$ eV, $\lambda_s = 0.5$ eV. [e] $H_j = (8\pi^2 F_j V^2 \tau_L)/h\lambda_s$ adiabaticity parameter; $V = 1000$ cm^{-1} except those marked with * where $V = 250$ and 100 cm^{-1}, respectively, and $\tau_L = 0.5$ ps. [f] $0 \rightarrow$ j BET rate: see eq 4a. [g] Porphyrin/bacteriopheophytin pair, see: Laporte, L.; McDowell, L. M.; Kirmaier, C.; Schenck, C. C.; Holten, D. *Chem. Phys.* **1993**, *176*, 615. [h] $\lambda_v = 0.1$ eV, $h\nu_v = 1500$ cm^{-1}. [i] $\Delta G = -1.24$ eV, $\lambda_s = 0.2$ eV. [j] Adiabaticity parameter; $V = 1000$ cm^{-1} except *, $V = 250$ cm^{-1}, $\tau_L = 0.5$ ps. [k] $0 \rightarrow$ BET rate.

represented by an electronic transmission coefficient $\kappa_{el} \approx 1$) is governed by the ratio of the energy gap to the total reorganization energy, $\lambda_s + \lambda_v$.

1. $\lambda_{v.}$ The internal reorganization energy for the outer-sphere ET reaction maybe expressed in terms of the Marcus cross-relation[8a]

$$\lambda_v = \frac{(\lambda_P + \lambda_{UQ_0})}{2} \tag{2}$$

where λ_P and λ_{UQ_0} are the internal reorganizations associated with the self-exchange ET reactions for P and UQ_0, respectively. λ_P is expected to be relatively small as can be inferred from the modest frequency changes upon oxidation. In the reaction center, the reorganization energy attributed to the porphyrin tetrapyrrole groups of the bacteriochlorophyll/bacteriopheophytin donor−acceptor pair is relatively small ($\lambda_v \approx 0.1$ eV).[30] In contrast, large changes in the ubiquinone vibrational spectrum as well as bond length changes (Table 2) (between the neutral and anionic species) indicate a substantial λ_{UQ_0}. Traditionally, evaluation of λ_v has relied on a knowledge of force constants and atomic coordinates of the neutral and charged species.[31] While it is clear that the largest changes in the $UQ_0/UQ_0^{\bullet-}$ spectra involve normal modes with predominat contributions from C═O stretching motions,[29] the absence of a complete normal-mode analyses and the rarity of crystal structure data on organic radical ions makes the quantitative determination of λ_{UQ_0} difficult. Thus, to obtain λ_{UQ_0} we turn to the ab initio energy calculations. The method used here and illustrated in Figure 6 is similar to that originally utilized by Larsson et al.[32] Figure 6 represents potential energy surfaces corresponding to the hypothetical gas-phase reaction $UQ_0^{\bullet-} \rightleftharpoons UQ_0 + e^-$. $E(UQ_0)$ and $E(UQ_0^*)$ represent the total electronic energies of the neutral ubiquinone calculated at its equilibrium geometry and at the equilibrium geometry of the radical anion, respectively. The total energies of the radical anion calculated at its equilibrium geometry and at the equilibrium geometry of the neutral are represented by $E(UQ_0^{\bullet-})$ and $E(UQ_0^{\bullet-*})$. The vertical ionization energy of $UQ_0^{\bullet-}$ (a in Figure 6) is equal to the sum of the energy ($\Delta E°$) and the reorganization energy (λ_{ET}) of the process analogous to the forward ET process. The difference between the adiabatic electron affinity of UQ_0 (b in Figure 6) and the vertical electron affinity (c in Figure 6) represents λ_{BET} localized at the ubiquinone moiety. While the usual theories of electron-transfer rates assume parabolic potential energy surfaces with equal force constants to describe reactants and products,[33] differences in frequencies and force constants (between reactant and product surfaces) are implied in the numerically different values of $\lambda_{ET} \approx 0.64$ and $\lambda_{BET} \approx 0.53$ eV. In keeping with the basic tenets of the theories of ET used in the discussion that follows we have averaged the two reorganizational energies; hence, $\lambda_{UQ_0} \approx 0.60$ eV. However, a small difference between the two large numbers to generate λ_{UQ_0} intrinsically raises concerns about the correctness of the value. One way to validate the accuracy of the calculations is to compare the agreement between experimentally available parameters such as the adiabatic electron affinity on related systems, which is also obtained in parallel with λ_{UQ_0}. The value obtained here is in good agreement with published data.[19a,34] Furthermore, the good agreement of the geometrical information (with published X-ray data for the neutral),[35] including the vibrational frequencies, with experimental data,[29] gives us confidence in our calculated energies associated with these geometries.

2. λ_s. Because of its small size, UQ_0 makes even more substantial contribution to the solvent reorganization than the bigger porphyrin. The standard estimate of solvent reorganization has been achieved via the dielectric continuum model of Marcus.[8a] Two forms are familiar: one that considers reactants as two nonoverlapping spheres and the other being the dipole in a sphere (of radius a) scheme.[36] For the $P^{\bullet+}/UQ_0^{\bullet-}$ complex the latter model as shown in eq 3 is more appropriate as it precludes a solvent layer between the contact pair complex assumed here.[18a]

$$\lambda_s = \frac{(\Delta\mu)^2}{a^3}(f(D_{op}) - f(D_s))$$

$$f(D) = -\frac{D-1}{2D+1} \tag{3}$$

$\Delta\mu$ denotes the vector difference of dipole moments between the initial and final electronic states, while D_{op} represents the index of refraction of water squared and D_s is the static dielectric constant of water, the solvent used here. From an assumed spherical radius of 5 Å (average of P and UQ_0 radii of ≈7 and ≈ 3Å, respectively), a separation of 3.3 Å for a contact pair [37] (and thus giving an upper limit estimate of $\Delta\mu \approx 16$D), λ_s is calculated to be about 0.50 eV.[38]

3. Electron-Transfer Kinetics. The BET process in this work appears to be extremely fast as implied by the absence of long-

lived ($\tau \ll$ ns) charge-transfer products (vide supra). To make a clear argument for the efficient mediation of rapid BET by vibrational overlap factors evaluated above, we turn to theories of electron transfer. Electron-transfer formalisms are often cast in terms of their adiabaticity.[8a,39] The conventional representation associates adiabaticity with a large value of the electronic matrix element, (e.g., $k_BT \ll V$), while nonadiabaticity is implied by a small V (e.g., $V \ll k_BT$). In the present study, a large value of V is expected, given the spin-allowed nature of BET from a contact pair. A theoretical expression for ET rates, which bridges the nonadiabatic and the solvent-controlled adiabatic limits, has been derived by Jortner et al. [40] This is shown in eq 4, in the formalism used by Gould, Young, and Farid et al. [37b] The $(1 + H_j)^{-1}$ "adiabaticity" factor keeps the rate reasonably finite when V is big. Thus, in the nonadiabatic limit (i.e., when $H_j \ll 1$) eq 4a collapses to the normal golden rule type formula, [39b] and when $H_j \gg 1$ eq 4 transforms into the "solvent-controlled" adiabatic limit where the putative rate is assumed to be curbed[41] by the solvent longitudinal relaxation time, τ_L^{-1} (water) ≈ 1.9 ps^{-1}.[42] In eq 4a the Franck−Condon factor consists of the sum over all possible vibrational overlap factors (F_j) between a single initial vibrational level $i = 0$ and final j level for a single high-frequency mode $h\nu_v$ (e.g., 1500 cm^{-1}).[37] The $0 \rightarrow j$ transitions are accompanied by transitions to low-frequency modes commonly associated with λ_s. Thus, each summand represents a separate $0 \rightarrow j$ BET pathway, with its $\Delta G_{BET} + jh\nu_v$ contributing to the total rate.

$$k_{BET} = \left(\frac{4\pi^3}{h^2\lambda_s k_B T}\right)\sum_{j=0}^{\infty}\frac{F_j V^2}{(1+H_j)}\exp\left\{\frac{-(\lambda_s + jh\nu_v + \Delta G_{BET})^2}{4\lambda_s k_B T}\right\} \quad (4a)$$

$$F_j = \frac{e^{-s}S^j}{j!}; \quad S = \frac{\lambda_v}{h\nu_v} \quad (4b)$$

$$H_j = \frac{8\pi^2 F_j V^2 \tau_L}{h\lambda_s} \quad (4c)$$

Table 4 contains a listing of Franck−Condon factors (F_j, κ_j) and k_{BET} for $0 \rightarrow$ 1,2,3, ..., 7 BET transitions for the $P^{\bullet+}/UQ_0^{\bullet-}$ and $P^{\bullet+}/BPh^{\bullet-}$ pairs.[43] The latter pair ($\lambda_s \approx 0.2$ eV is estimated from eq 3 for $a \approx 7$ Å and $\lambda_v \approx 0.1$ eV [30]) is given as a contrast to check the extent of the influence of the structural changes, mainly associated with UQ_0, on mediating efficient BET. For $P^{\bullet+}/UQ_0^{\bullet-}$, six of the eight channels considered, it is clear that F_j and the Marcus exponential activation term (κ_j) both combine to favor efficient BET, whereas in the $P^{\bullet+}/BPh^{\bullet-}$ case, for a given summand, a favorable F_j is invariably offset by a mismatch due to a barrier associated with κ_j and vice versa. This is a consequence of the $P^{\bullet+}/BPh^{\bullet-}$ system being deep in the inverted region, $|\Delta G| > \lambda$, where the absence of reactant/product potential surface crossing leads to poor vibrational Franck−Condon overlaps.[44]

To complete the discussion, it is useful to obtain rate constants. This requires a reasonable estimate of V. The contact pair $P^{\bullet+}/UQ_0^{\bullet-}$ complex is expected to be strongly coupled; thus, a value of $V \approx 1000$ cm^{-1} based on experimental figures for contact pairs in aromantic organic systems [37,45] is not out of the question. In this high-coupling limit, the j specific rates for the $P^{\bullet+}/UQ_0^{\bullet-}$ pair are all large with the three and four channels close to the solvent limit. In contrast, in the $P^{\bullet+}/BPh^{\bullet-}$ dyad, only the $0 \rightarrow 5$ transition is close to the fast channels, i.e., $0 \rightarrow$ 1,2, ..., 6 of the $P^{\bullet+}/UQ_0^{\bullet-}$ pair. There is, however, a notable distinction; the fast channels of the latter are adiabatic ($H_j \gg 1$) while the fastest channel ($0 \rightarrow 5$) of $P^{\bullet+}/BPh^{\bullet-}$, is nonadiabatic ($H_j = 0.2$). As a result, BET efficiency for the $P^{\bullet+}/BPh^{\bullet-}$ model is sensitive to changes in the magnitude of the electronic matrix element, while $P^{\bullet+}/UQ_0^{\bullet-}$s fastest channels are likely to maintain about the same BET rates as long as they remain adiabatic with changes in V. Accordingly, if V was diminished to 250 and 100 cm^{-1}, the net effect on the $0 \rightarrow 5$ transition of $P^{\bullet+}/BPh^{\bullet-}$ is a respective decrease of 1 and 2 orders of magnitude from the rate of 6.4×10^{10} s^{-1}, while $P^{\bullet+}/UQ_0^{\bullet-}$'s $0 \rightarrow 3$ transition changes from 1.0×10^{12} s^{-1} at $V = 1000$ cm^{-1} to 8.3×10^{11} s^{-1} and 3.5×10^{11} s^{-1} for $V = 250$ and 100 cm^{-1}, respectively. These results demonstrate that in the case of $P^{\bullet+}/BPh^{\bullet-}$, very poor Franck−Condon factors for BET must rely on moderate to small V's (e.g., $\leq kT$) to effectively mediate efficient charge separation. The structural distortions of UQ_0 in the present model system lead to very favorable Franck−Condon factors for BET, which in the absence of spin multiplicity changes (e.g., triplet-state correlated ET [12]) charge separation cannot compete with BET.

VI. Conclusions

Excited porphyrin singlet-correlated products of photoinduced ET are clearly observed using TRRS. Generally the spectra of the transient $P^{\bullet+}$ species correspond to those of free ions that have been generated chemically in situ or electrochemically. The spectra of $UQ_0^{\bullet-}$ reveals features consistent with the acceptor being perturbed by the proximate $P^{\bullet+}$ donor, notably the 1435 cm^{-1} stretch.

Electronic structure and geometry calculations for the ubiquinone acceptor have been performed. The vibrational data were used to assign the various vibrational frequencies of ubiquinone. The internal reorganization energy for adding an electron to the neutral UQ_0 and for removing the electron from the $UQ_0^{\bullet-}$ radical anion was calculated. Subsequent analysis of energy structure calculations of $UQ_0/UQ_0^{\bullet-}$ reveal important general considerations for the study of simple ET model systems from the perspective of charge separation. The structural distortion undergone by UQ_0 or a similar acceptor is sufficiently large, that *spin-allowed* BET can only be frustrated by unrealistically small values of V. This, of course, is not a problem if changes in spin multiplicity changes occur.[12,45] Furthermore, in cases where the vibrational overlaps are determined to be favorable for charge separation, careful consideration must be given to electronic coupling, as a favorable V and other factors may still negate any putative Franck−Condon barriers to BET.[46]

Acknowledgment. This work was supported by the NIH (GM 33330). We acknowledge useful discussions with Drs. Vince Ortiz, Ralph Young, John Endicott, Martin Kirk, and Ms. Rebecca Emeny.

Supporting Information Available: Tables of calculated vibrational frequency, structure, and energy data on ubiquinone using BLYP/6−3G* basis sets (5 pages). Ordering and access information is given on any current masthead.

References and Notes

(1) A preliminary account of this work has appeared in the following: Buranda, T.; Soice, N.; Greiner, J.; Prajakrattanajakij, S.; Ondrias M. *In The Proceedings of the Fifteenth International Conference on Raman Spectroscopy*; Asher, S. A., Stein, P., Eds.; John Wiley & Sons: Chichester, England, 1996; p 134.

(2) For reviews, see: (a) Fox, M. A., Chanon, M. Eds. *Photoinduced Electron Transfer;* Elsevier: Amsterdam, 1988; Parts A−D. (b) Balzani,

V.; Scandola, F. *Supramolecular Photochemistry;* Simon and Schuster: Heme Hempstead, England, 1990. (c) Barbara, P. F.; Meyer, T. J.; Ratner, M. A. *J. Phys. Chem.* **1996,** *100,* 13148.

(3) (a) *The Photosynthetic Reaction Center Complex: Structure and Dynamics;* Breton, J.; Vermiglio, A. Eds.; Plenum Press: New York, 1988. (b) Plato, M.; Mobius, K.; Michel-Beyerle, M. E.; Bixon, M.; Jortner, J. *J. Am. Chem. Soc.* **1988**, *110,* 7279. (c) Franzen, S.; Goldstein, R. F.; Boxer, S. G. *J. Phys. Chem.* **1993,** *97,* 3040.

(4) (a) Gust D.; Moore, T. A.; Moore, A. L. *Acc. Chem. Res.* **1993**, *26* 198. (b) Wasielewski, M. R. *Chem. Rev.* **1992**, *92,* 435.

(5) (a) Turro, C.; Chang, C. K.; Leroi, G. E.; Cukier, R. I. Nocera, D. G. *J. Am. Chem. Soc.* **1992**, *114,* 4013. (b) D'Souza, F. *J. Am. Chem. Soc.* **1996**, *118,* 923. (c) Hayashi, T.; Miyahara, T.; Hashizume, N.; Ogoshi, H. *J. Am. Chem. Soc.* **1993,** *115,* 2049.

(6) (a) Harriman, A.; Magda, D. J.; Sessler, J. L. *J. Phys. Chem.* **1991,** *95,* 1530. (b) Harriman, A.; Kubo, Y.; Sessler, J. L. *J. Am. Chem. Soc.* **1992,** *114,* 388.

(7) (a) For extensive literature on related bimolecular ET processes, see: Kalyanasundaram, K. *Photochemistry of Polypyridine and Porphyrin Complexes*; Academic Press: New York, 1992; pp 450−478 and references therein. (b) Hug, G. L.; Marciniak, B.; *J. Phys. Chem.* **1995**, *99,* 1478 and references therein. (c) Logunov, S. L.; Rodgers, M. A. J. *J. Photochem. Photobio. A* **1997,** *105,* 55−63.

(8) (a) Marcus, R. A.; Sutin, N. *Biochim. Biophys. Acta* **1985**, *811,* 265. (b) Gunner, M. R.; Dutton, P. L. *J. Am. Chem. Soc.* **1989**, *111,* 3400−3412. (c) Jortner, J. *J. Am. Chem. Soc.* **1980,** *102,* 6676. (d) Franzen, S.; Goldstein, R. F.; Boxer, S. G. *J. Phys. Chem.* **1990,** *94,* 5135.

(9) Mataga, N.; Karen, A.; Okada, T.; Nishitani, S.; Sakata, Y.; Misumi. *J. Phys. Chem.* **1984**, *88,* 4650.

(10) (a) Holten, D.; Gouterman, M.; Parson, W. W.; Windsor, M.; Rockley, M. G. *Photochem. Photobiol*. **1976**, *23*, 415. (b) Gouterman, M.; Holten, D. *Photochem. Photobiol.* **1977**, *25*, 85.

(11) Kalyanasundaram, K.; *Photochemistry of Polypyridine and Porphyrin Complexes*; Academic Press: New York, 1992; p 420.

(12) Buranda, T.; Soice, N.; Niu, S.; Larsen, R.; Ondrias, M. *J. Phys. Chem*. **1996**, *100,* 18868.

(13) Benisi, H. A.; Hilderbrand, J. H. *J. Am. Chem. Soc*. **1948,** *70,* 3978.

(14) (a) Simpson, M. C.; Peterson, E. S.; Shannon, C. F.; Eads, D. D.; Friedman, J. M.; Cheatum, C. M.; Ondrias, M. R. *J. Am. Chem. Soc.* **1997**, *119,* 5110. (b) Schneerbeck, M. C.; Vigil, L. E.; Ondrias, M. R. *Chem. Phys. Lett.* **1993,** *215,* 251. (c) Wall, M. H.; Basu, P.; Buranda, T.; Wicks, B. S.; Findsen, E. W.; Ondrias, M. R.; Enemark, J. H.; Kirk, M. L. *Inorg. Chem.* **1997**, *36*, 5676.

(15) Frisch, M. J.; Trucks, G. W.; Schlegel, H. B.; Gill, P. M. W.; Johnson, B. G.; Robb, M. A.; Cheeseman, J. R.; Keith, T.; Petersson, G. A.; Montgomery, J. A.; Raghavachari, K.; Al-Laham, M. A.; Zakrzewski, V. G.; Ortiz, J. V.; Foresman, J. B.; Cioslowski, J.; Stefanov, B. B.; Nanayakkara, A.; Challacombe, M.; Peng, C. Y.; Ayala, P. Y.; Chen, W.; Wong, M. W.; Andres, J. L.; Replogle, E. S.; Gomperts, R.; Martin, R. L.; Fox, D. J.; Binkley, J. S.; Defrees, D. J.; Baker, J.; Stewart, J. P.; Head-Gordon, M.; Gonzalez, C.; Pople, J. A. *Gaussian 94*, Revision D.4; Gaussian, Inc.: Pittsburgh, PA, 1995.

(16) (a) Becke, A. D. *Phys. Rev. A.* **1988**, *38,* 3098. (b) Lee, C.; Yang, W.; Parr, G. *Phys. Rev. B.* **1988**, *37,* 785. (c) Pople, J. A.; Schlegel, H. B.; Krishnan, R.; Defrees, D. J.; Binkley, J. S.; Frish, M. J.; Whitside, R. A.; Hout, R. F.; Hehre, W. J. *Int. J. Quantum Chem.* **1981**, *S15,* 269.

(17) Molden, Version 3.0: G. Schaftenaar.

(18) (a) The π systems of the P and UQ_0 complexed pair are assumed to be stacked in a face-to-face configuration; thus, the π orbital interaction mediates ET quenching, see: (b) Sato, T.; Ogawa, T.; Kano, K. *J. Phys. Chem.* **1984,** *88,* 3678−3682. (c) Shelnutt, J. A. *J. Phys. Chem.* **1984,** *88,* 6121. (d) Brun, A. M.; Harriman, A.; Hubig, S. *J. Phys. Chem.* **1992**, *96*, 254.

(19) (a) Boesch, S. E.; Grafton, A. K.; Wheeler, R. A. *J. Phys. Chem*. **1996,** *100,* 10083. (b) Balakrishnan, G.; Pothukattil, M.; Umapathy, S. *Spectrochim. Acta A* **1997**, *53*, 1553−1561 (c) Balakrishnan, G.; Pothukattil, M.; Umapathy, S. *J. Phys. Chem.* **1996**, *100*, 16472. (d) Chipman D. M.; Prebenda M. F. *J. Phys. Chem.* **1986**, *90*, 5557−5560.

(20) (a) Gouterman, M. In *The Porphyrins*, Dolphin. D., Ed.; Academic Press: New York, 1978; Vol. II, p 1. (b) Dolphin, D., Ed.; *The Porphyrins*; Academic Press: New York, 1978; Vols. I−V. (c) Rodriguez, J.; Kirmaier, C. Holten, D. *J. Am. Chem. Soc.* **1989,** *111,* 6500.

(21) (a) Czernuszewicz, R. S.; Macor, K. A.; Li, X.; Kincaid, J. R.; Spiro, T. G.; *J. Am. Chem. Soc*. **1989**, *11*, 3860−3869. (b) Oertling, W. A.; Salehi, A.; Chang, A. K.; Babcock, G. T. *J. Phys. Chem.* **1989**, 93, 1311−1319. (c) Reed, R. A.; Purrello, R.; Prendergast, K.; Spiro, T. G. *J. Phys. Chem.* **1991**, *95*, 9720−9727. (d) de Paula, J. C.; Walters, V. A.; Nutaitis, C.; Lind, J.; Hall, K.; *J. Phys. Chem.* **1992,** *92*, 10591−10594. (e) Walters, V. A.; de Paula, J. C.; Babcock, G. T.; Leroy, G. E. *J. Am. Chem. Soc.* **1989**, *111*, 8300−8302. (f) Kumble, R.; Hu, S.; Loppnow, G. R., Vitols, S. E.; Spiro, T. G. *J. Phys. Chem.* **1993**, *97*, 10521−10523.

(22) (a) McMahon, R. J.; Force, R. K.; Patterson, H. H.; Wrighton, M. S. *J. Am. Chem. Soc.* **1988**, *110*, 2670. (b). Fuchs, M.; Vongersdorff, J.; Dieks, H.; Kurreck, H.; Mobius, K.; Prisner, T. *J. Chem. Soc., Faraday Trans.* **1996,** *92*, 949−955.

(23) The reaction free energies were determined from $\Delta G_{ET} = (E_{ox} - E_{red}) - E_{singlet} - E_{Coulombic}$ (see Rehm, D.; Weller, A. *Isr. J. Chem.* **1970**, *8*, 259), $E_{ox} = 0.6$ eV, $E_{red} = -0.55$ eV, $E_{singlet} = 1.8$ eV, $E_{Coulombic} \approx 0.05$ eV, $-\Delta G_{BET} = (E_{ox} - E_{red})$.

(24) (a) Beck, S. M.; Brus L. E. *J. Am. Chem. Soc*. **1982**, *104*, 1103. (b) Beck, S. M.; Brus, L. E. *J. Am. Chem. Soc*. **1982,** *104*, 4789.

(25) (a) *The Chemistry of Quinonoid Compounds;* Patai, S., Rappaport, Z., Eds. Wiley and Sons: New York, 1988; Vol. II. (b) Burie, J.; Boussac, A.; Boullais, C.; Berger, G.; Mattioli, T.; Mioskowski, C.; Nabedryk; Breton, J. *J. Phys. Chem.* **1995**, *99*, 4059 (c) Buesch, S. E.; Wheeler, R. A. *J. Phys. Chem.* **1997**, *101*, 5799−5804.

(26) Parker, A. W.; Hester, R. E.; Phillips, D.; Umapathy, S. *J. Chem. Soc., Faraday Trans.* **1992**, *88*, 2649.

(27) Swallow, A. J. In *Function of Quinones in Energy Conserving Systems;* Trumpower, B. L., Ed.; Academic Press: New York, 1982; p 59.

(28) Bauscher; M.; Mantele, W. *J. Phys. Chem.* **1992**, *96*, 11101.

(29) (a) Breton, J.; Boullais, C.; Burie, J.; Nabedryk, E.; Mioskowski, C. *Biochemistry* **1994**, *33*, 14378. (b) Hienerwadel, R.; Thibodeau, D.; Lenz, F.; Breton, J.; Nabedryk, E.; Kreutz, W. Mäntele. In *Time-Resolved Vibrational Spectroscopy V*, Takahashi, H., Ed.; Springer−Verlag: Berlin, Heidelberg, 1992; p 83−86.

(30) Warshel, A. *Proc. Natl. Acad. Sci. U.S.A.* **1980,** *77*, 3105.

(31) Recently other methods depending on the analysis of resonance Raman profiles of charge-transfer absorption bands as a way of obtaining reorganization energies have been have been published, e.g.: (a) Markel, F.; Ferris, N. S.; Gould, I. R.; Myers, A. B. *J. Chem. Soc*. **1992**, *114*, 6208. (b) Kulinowski, K.; Gould, I. R.; Myers, A. B. *J. Phys. Chem.* **1995,** *99*, 9017. (c) Doorn S. K.; Hupp, J. T. *J. Am. Chem. Soc.* **1989**, *111*, 1142.

(32) Klimkans, A.; Larsson, S. *Chem. Phys.* **1994**, *189*, 25.

(33) Ulstrup, J.; Jortner, J. *J. Chem. Phys.* **1975,** *63*, 4358

(34) (a) Fukuda, E. K.; McIver, R. T. J. *J. Am. Chem. Soc.* **1985**, *107*, 2291−2296. (b) Jaworski, J. S. *Chem. Phys. Lett.* **1986,** *127*, 133. (c) Unpublished data of Wheeler et al. gives an upper estimate of the reorganization energy of ubiquinone-1 of ≈0.69 eV using hybrid Hartree−Fock/density-functional approaches with large basis sets.

(35) (a) Siverman, J.; Stam-Thole, I.; Stam, C. H. *Acta Crystallogr. B* **1971**, *27*, 1846−1851. (b) Schmalle, H. W.; Jarchow, O. H. Hausen, B. M.; Shultz, K. H. *Acta Crystallogr. C* **1984**, *40*, 1090−1092.

(36) Marcus, R. A. *J. Phys. Chem.* **1990,** *94*, 4963.

(37) (a) Gould, I. R.; Farid, S. Young, R. H. *J. Photochem. Photobiol. A* **1992**, *65*, 133 (b) Gould, I. R.; Young, R. H.; Moody, R. E.; Farid; S. *J. Phys. Chem.* **1991,** *95*, 2068−2028.

(38) While this value is in good agreement with experimental numbers for related systems,[7c,37] the dielectric continuum model is limited by the assumed spherical geometry of flat molecules. The redistributions of electron density with apparent charge localizations at the C═O groups (as implied by the local charge density shown by the Muliken population analysis (Table 4)) cannot be accounted for by the model. Other shortcomings of the dielectric contiuum model, such as failure to account for polarization and hydrogen-bonding effects, have recently been reviewed.[2c] However, it is important to note that in spite of these shortcomings the dielectric continuum model has been remarkably successful in the estimation of λ_s.

(39) (a) Newton, M. D.; Sutin, N. *Annu. Rev. Phys. Chem.* **1984,** *35*, 437 (b) Kestner, N. R.; Logan, J.; Jortner, J. *J. Phys. Chem.* **1974,** *78*, 2148.

(40) (a) Rips, I.; Jortner, J. *J. Chem. Phys*. **1987,** *87*, 2090. (b) Jortner, J.; Bixon, M. *J. Chem. Phys.* **1988,** *88*, 167.

(41) Rates exceeding the τ_L^{-1} limit have been reported e.g.: Åkesson, E.; Walker, G. C.; Barbara, P. F. *J. Chem. Phys.* **1991**, *91*, 4188. Åkesson, E.; Johnson, A. E.; Levinger, N. E.; Walker, G. C.; DuBruil, T. B.; Barbara, P. F. *J. Chem. Phys.* **1992,** *96*, 7859. In the case of the inverted region where no "classical barrier crossing" exists, excited-state relaxation occurs from multiple vibrational states, and thus the BET rate is weakly dependent on the medium relaxation dynamics represented by τ_L^{-1}. A similar situation obtains for activationless processes; for a good discussion, see: Bixon, M.; Jortner, J. *Chem. Phys.* **1993,** *176*, 467.

(42) Weaver, M. J.; McManis, G. E. *Acc. Chem. Res.* **1990,** *23*, 294.

(43) Laporte, L. McDowell, L. M.; Kirmaier, C.; Schenck, C. C.; Holten, D. *Chem. Phys.* **1993,** *176*, 616.

(44) Henry, B. R.; Siebrand, W. In *Organic Molecular Photophysics*; Birks, J. B., Ed.; Wiley: New York, 1975; Vol. 1, p 196.

(45) (a) Buranda, T.; Lei, Y.; Endicott, J. F. *J. Am. Chem. Soc.* **1992,** *114*, 6916. (b) Newton, M. D. *Chem. Rev.* **1991**, *81*, 767 and references therein. (c) Endicott, J. F. *Acc. Chem. Res.* **1988**, *21*, 59. (d) Endicott J. F.; Watzky, M. A.; Song, X.; Buranda, T. *Coord. Chem. Rev.* **1997**, *159*, 295.

(46) From the viewpoint of designing better models for charge separation, Holten et al. have concluded that the manipulation of Franck−Condon factors through the energy gap may have the undesired effect of activating "indirect electronic couplings and thermal activation routes that may enhance rather than hinder the competing deactivation pathways".[43]